Computational and Theoretical Chemistry 983 (2012) 31–37

Contents lists available at SciVerse ScienceDirect

Computational and Theoretical Chemistry

journal homepage: www.elsevier.com/locate/comptc

Mechanistic and kinetic study on the reaction of 2;4-dibrominated diphenyl ether (BDE-7) with OH radicals

Haijie Cao [a], Maoxia He [a,*], Dandan Han [a], Yanhui Sun [a], Sufang Zhao [b], Hongjuan Ma [b], Side Yao [b]

[a] Environment Research Institute;Shandong University;Jinan 250100;PR China
[b] Shanghai Institute of Applied Physics, Chinese Academy of Sciences, PO Box 800-204, Shanghai 201800, PR China

ARTICLE INFO

Article history:
Received 23 July 2011
Received in revised form 23 December 2011
Accepted 23 December 2011
Available online 14 January 2012

Keywords:
BDE-7
OH radicals
Reaction mechanism
Rate constants
Theoretical study

ABSTRACT

The mechanism and kinetic properties of OH-initiated gas-phase reaction of 2,4-dibrominated diphenyl ether (BDE-7) were studied at the MPWB1K/6-311+G(3df,2p)//MPWB1K/6-31+G(d,p) level of theory. Two types of reactions, hydroxyl addition and hydrogen abstraction, were investigated. The calculation results indicate that addition reactions, except for the bromo-substituted one, have lower barriers than hydrogen abstraction reactions. Moreover, hydroxyl radicals are likely to react with phenyl ring without bromine atoms. Rate constants were deduced over 200–1000 K using canonical variational transition state theory with small curvature tunneling contribution. At 298 K the calculated rate constant for the title reaction is 3.76×10^{-12} cm^{-3} molecule^{-1} s^{-1}.

1. Introduction

Polybrominated diphenyl ethers (PBDEs), a class of the brominated flame retardants (BFRS), have become worldwide contaminants due to their heavy use. They were added to textiles, construction materials, electronic equipments and so on [1,2]. PBDEs do not bind chemically to manufactures which cause them to be released to the environment easily [3]. PBDEs have been detected widely in organism environment (red alga, fish, plasma and mammals) and abiotic environment (air, dust, water, snow, sediments and sewage sludge) [2,4–8]. Concentrations of PBDEs have increased gradually over the past decades.

Concern for toxity of PBDEs has been growing because of the high frequency of detection. So far, PBDEs are confirmed to bioaccumulate in organisms and biomagnify in the food chain [9,10]. Some PBDEs have been shown to be endocrine disruptors which cause neurodevelopmental toxic effects [11,12]. PBDEs, rather than other organohalogen compounds, are believed to be more potent thyroid disruptors. 2,2′,4,4′-tetraBDE (BDE-47) has been found to be harmful to the nervous system [13,14]. This effect will be strengthened when coupled with PCB-153. Penta-BDEs demonstrate thyroid hormone influence on future generations [15]. Octa-BDEs cause toxity and teratogenicity to fetus while deca-BDE is harmful to the memory of children.

BDE-7 has been detected in many kinds of samples [16,17]. Most BDE-7 in environment comes from debromination of high-brominated diphenyl ethers and it is found that BDE-47 also generates BDE-7 through photochemical reactions.

Although some studies on the photolytic degradation of PBDEs in solution and mix-phase process have been done [18–20], the investigation of the atmospheric chemistry of PBDEs is not sufficient. Information including thermodynamic (ex. thermal energy, enthalpy and reaction mechanism) and kinetic properties (ex. rate constants, branching ratios, etc.) should be obtained in order to accurately predict the real atmospheric effect of these reactions.

In this paper, BDE-7 is chosen as a typical compound of PBDEs. BDE-7, one of the low-brominated diphenyl ethers, is thought to be more volatile and thus will exist in gas phase. As we all know, PBDEs in the atmosphere can be removed and transformed through unimolecular reaction (debromination with light) and bimolecular reaction (reaction with OH, HO_2, NO_3 radicals and O_3 molecules). Generally, the debromination reactions are thought to proceed with the sun while bimolecular reaction will occur anyway. Moreover, the reaction of aromatic compounds with NO_3 is considered to be less important than that of OH [21]. So the focus of this paper is the reaction of BDE-7 with OH radicals. In addition, the products formed in OH-initiated reaction of PBDEs can further generate much more toxic halogenated dioxins. Therefore, it is of great significance to study the reaction mechanism of OH with PBDE. The previous work of our groups has shown detailed gas phase mechanism for reaction of hydroxyl radicals with BDE-47 [22] and the total rate constant for the initial step has been given as 8.29×10^{-13} cm^{-3} molecule^{-1} s^{-1}. Zhou et al. [23] computed the rate constants of BDE-15 and OH. Their calculated value was 7.02×10^{-12} cm^3 molecule^{-1} s^{-1} at 298 K. Raff and Hites [24] determined the

* Corresponding author. Fax: +86 531 8836 9788.
E-mail address: hemaox@sdu.edu.cn (M. He).

2210-271X/$ - see front matter © 2012 Elsevier B.V. All rights reserved.
doi:10.1016/j.comptc.2011.12.017

rate constants for the gas-phase reactions of OH radicals with diphenyl ether and several polybrominated diphenyl ethers with 0–2 bromines. The results revealed that rate constants showed negative dependence on halogen degrees of PBDEs. Rate constants for the title reactions are around 3.88×10^{-12} cm^{-3} molecule^{-1} s^{-1} at 298 K. However, this experimental value may contain some inaccuracy due to the interruption of secondary reaction. Furthermore, collision is another remove path of detected substance, which causes inaccuracy in detection.

The aim of this study is to thoroughly investigate the reaction mechanism and rate constants over a wide range of temperature for the reaction of OH with BDE-7 using quantum chemical method. This method can accurately calculate the reaction energy barrier, the enthalpies of formation and the rate constants. By using these data, the detailed potential energy surface and completed reaction mechanism can be proposed. We expect this work could be a supplement to experimental study and an attempt to theoretical investigation of the OH-initiated photochemical reaction mechanism of PBDEs.

2. Computational methods

All the geometries, frequencies and single point energies were performed using Gaussian 03 package [25]. Both DFT and MP2 methods are employed to obtain the energies. Geometry optimization was executed using MPWB1 K functional [26] which was developed specifically for kinetic applications and has shown to yield satisfying results in performing the interactions of van der Waals bond in the previous work [22,27–35]. The structures of stationary points (reactants, intermediates, transition states and products) were calculated at MPWB1K/6-31+G(d,p) level of theory. Frequencies and zero energy for the stationary points were obtained at the same level with optimizing step. In order to study the accuracy of the quantum methods, the MPWB1 K functional structures were then employed in single-point energy calculations by B3LYP functional and MØller-Plesset perturbation theory (MP2) with the same basis sets of 6-311+G(3df,2p). Intrinsic reaction coordinate (IRC) [36] calculations were performed for each transition states to verify the reaction pathways. Single point energies of the optimized structures were calculated with the level of MPWB1 K/6-311+(3df, 2p) to improve the calculation of barrier heights. In order to calculate the reactivity of reactants, molecule orbital interactions were also investigated at the level of MPWB1K/6-31+G(d,p).

Rate constants of each elementary step involved in this study were estimated using canonical variational transition-state (CVT) [37–39] theory. Quantum tunneling effects were performed using with small curvature tunneling (SCT) [40] method. The CVT rate constant for temperature T is given by:

$$k^{\mathrm{CVT}}(T,s)\min_{s} k^{\mathrm{GT}}(T,s) \tag{1}$$

where

$$k^{\mathrm{GT}}(T,s) = \frac{\sigma k_B T}{h}\frac{Q^{\mathrm{GT}}(T,s)}{\Phi^{R}(T)} e^{-V_{\mathrm{MEP}}(s)/(k_B T)} \tag{2}$$

Here k^{GT} (T, s) is the generalized transition state (GTS) theory rate constant at the dividing surface s, σ is the symmetry factor to illustrate the possibility of more than one symmetry-related reaction path. k_B is Boltzmann's constant, h is Planck's constant, $\Phi^{R}(T)$ is the reactants classical partition function per unit volume, and $Q^{\mathrm{GT}}(T, s)$ is the classical partition function of a generalized transition state at s with a local zero of energy at $V_{\mathrm{MEP}}(s)$ and with all rotational symmetry numbers set to unity. The kinetics calculations were carried out using POLYRATE 9.3 program [41].

3. Results and discussion

In the beginning of our study, we have chosen both DFT and ab initio method to study the accuracy of the quantum methods. As an example, MPWB1 K and MP2 have been chosen as respective methods of DFT and MP2 methods to calculate the reaction enthalpy of. The reaction enthalpies calculated on MPWB1 K, B3LYP and MP2 with 6-311+G(3df,2p) basis set are −13.53, −10.57 and −0.11 kcal/mol, respectively. Compared the calculated energies with experimental value (−14.62 kcal/mol) [42,43], we think the MPWB1 K method can give out satisfying results.

Two types of the title reactions including OH addition and hydrogen abstraction are discussed in this paper. The structure with atom labels of BDE-7 is shown in Scheme 1. The lowest energy structure has been chosen as the matrix for the following reactions. The dihedral angles of 6-1-7-1′ and 1-7-1′-2′ are 110.37° and −12.65°, respectively. Other parameters to determine the structure of BDE-7 are detailed in Scheme 1. With bromine atoms in the same phenyl, it is obviously that the two phenyl rings of BDE-7 are in different environments. Therefore, their reactions with OH should be studied separately.

3.1. Mechanism of reactions

Theoretically, two types of reactions will occur for the title reaction: one is OH-addition to phenyl ring and the other is OH abstraction of hydrogen or bromine on the phenyl ring. However, previous studies have shown that the bromine abstraction from PBDEs hardly occurs [24] and thus only OH-addition and hydrogen abstraction pathways are discussed in this paper. The schematic energetic profiles of the potential energy surface (PES) are plotted in Fig. 1a and b (a is for ring 1, b is for ring 2). Detailed reaction pathways of the title reaction are generated in Fig. 2. Geometries of transition states with selected parameters are shown in Fig. S1 In Supporting information. In order to facilitate description, phenyl ring with bromine atoms is defined as ring 1 while the other is ring 2. Detailed information of above reactions is given as follows.

3.1.1. Reaction pathways of ring 1

Twelve hydroxyl addition reactions are taken into consideration for the twelve types of carbon atoms in BDE-7. All these steps undergo similarly mechanism, that is, the attack of O of hydroxyl radical to carbon of ring1 and ring 2.

Firstly, hydroxyl radical can attack ipso carbon atom C(1) (pathway 1). This process needs to overcome a reaction energy barrier of 5.25 kcal/mol. The product P1 lies 22.99 kcal/mol below reactants. Secondly, O(8) atom may attack carbon atoms (C2 and C4) adjacent to Br atom, which leads to direct elimination of Br atoms as described in Fig. 2(pathway 2 and 4). Both pathways 2 and 4 are highly exothermic by −26.68 and −26.98 kcal/mol, respectively. However, the energy barrier of pathway 2 (7.06 kcal/mol) is lightly higher than that of pathway 4 (6.31 kcal/mol). This may be caused by steric hindrance. Finally, pathways 3, 5 and 6 undergo the reactions of OH being added to carbon atoms adjacent to hydrogen atoms. The barrier heights of above reactions are 3.47, 2.48 and 3.50 kcal/mol, respectively but they are less exothermic than

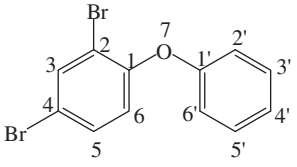

Scheme 1.

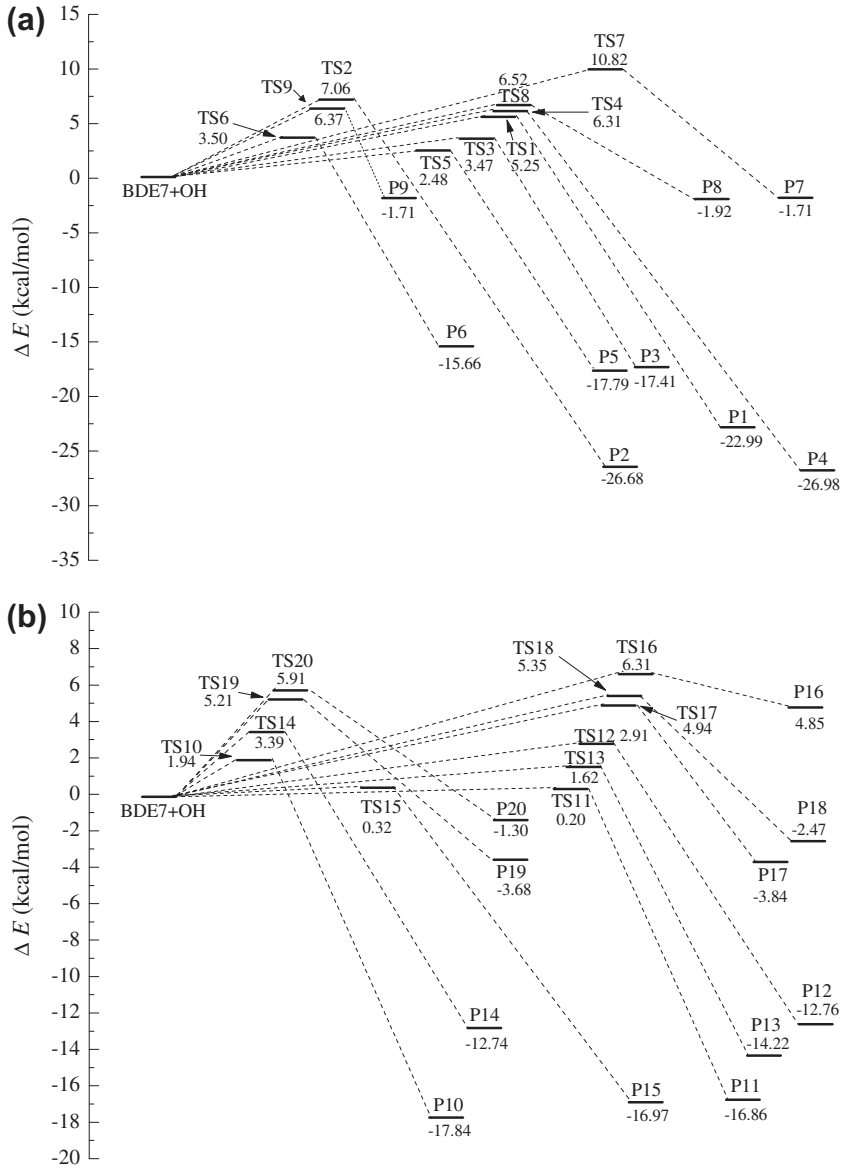

Fig. 1. Schematic energy diagrams predicted at the MPWB1K/6-311+G(3df,2p)//MPWB1K/6-31G(d) level of theory for the title reaction.

pathways 1, 2 and 4, which mean that their products (P2, P5 and P6) will definitely undergo other reactions to form stable products.

Phenyl hydrogen abstractions by hydroxyl radical have to pass over high energy barriers. TS7, TS8 and TS9 are their transition states with relative energy of 10.82, 6.52 and 6.40 kcal/mol respectively. Transition state TS7 is the abstraction of hydrogen adjacent to C(3). Bromine atoms in the same phenyl ring appear to generate steric hindrances which block hydrogen abstractions by hydroxyl radical. Products of pathway 7, 8 and 9 are water and unstable radicals (P7, P8 and P9). These pathways are slightly exothermic by 1.71, 1.91 and 1.71 kcal/mol, respectively.

3.1.2. Detailed mechanism of ring 2

Considering the conformation chosen in this paper, C(2′) and C(6′) atoms are not thought to be identical and neither were C(3′) and C(5′), and thus the five hydrogens on the Ring 2 are not identical. Therefore, the detailed properties of six hydroxyl addition and five hydrogen abstraction pathways are explored.

Pathway 10 is exothermic with −17.84 kcal/mol through a reaction barrier of 1.94 kcal/mol. Pathway 11 and 15 overcome similar reaction energy barriers (0.20 and 0.32 kcal/mol, respectively) and their products lie 16.86 and 16.96 kcal/mol below reactants, respectively. Pathway 12 and 14 are both exothermic (12.76 and 12.74 kcal/mol) while pathway 12 undergoes lower reaction energy barrier (2.91 kcal/mol) than pathway 14 (3.39 kcal/mol) does. Finally, approach of hydroxyl and C(4′) has to cross a barrier of 1.62 kcal/mol. Energy of its product (P14) is 14.22 kcal/mol below reactants.

For ring 2, phenyl hydrogen abstraction by hydroxyl radical seems to overcome higher reaction energy barriers than hydroxyl addition paths do. Moreover, these elementary reactions release less energy. Detailed reaction barriers and reaction enthalpies of pathway 16–20 are shown in Fig. 2.

Compared to pathways 7, 8 and 9, pathways 16–20 need cross lower reaction energy barriers while releasing more energy. Among all the hydrogen abstraction pathways, pathway 19 is the prior reaction with a barrier of 4.94 kcal/mol coupled with the most exothermicity of 3.84 kcal/mol. It is worth noting that product (P20) of pathway 20 lies 4.85 kcal/mol above reactants.

For the OH radical addition reactions, the C–O(7) bond lengths are between 1.935–1.983 Å. Also, hydrogens of hydroxyl radicals tend to point to center of relative phenyl ring except pathways 1 and 10.

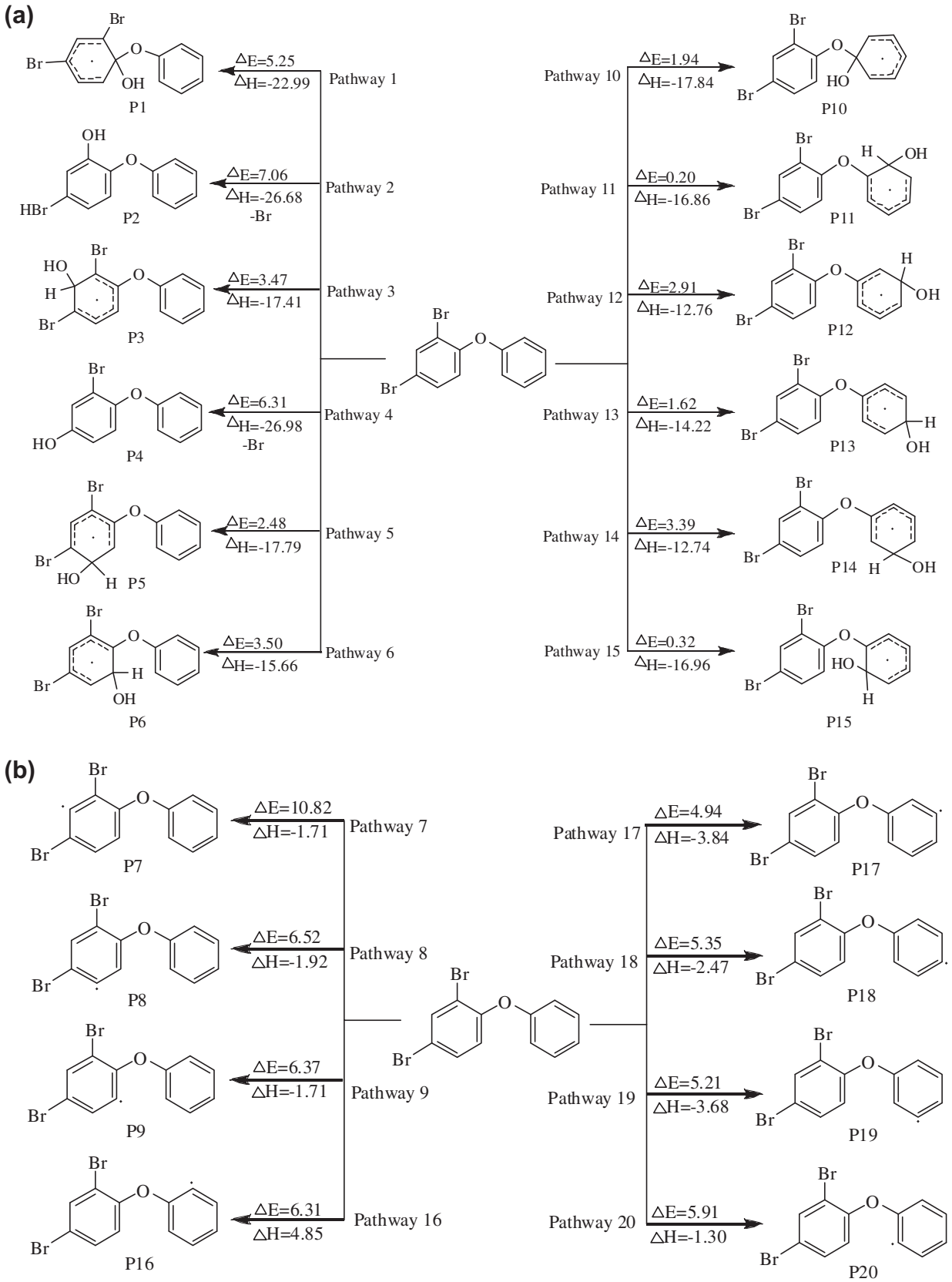

Fig. 2. Detailed reaction pathways of the title reaction. ΔE represents the energy barrier of each elementary reaction while ΔH stands for the reaction enthalpy.

By comparing the above calculated results, we conclude that hydroxyl addition reactions are more predominant than abstraction ones. Furthermore, the energy barriers for reactions that happened on ring 2 were lower compared to corresponding pathways of ring 1. But there is an exception for C(5) and C(5′). This phenomenon may be generated by the location of C(5) (Para

position of Br(2) and ortho position of Br(4)). For ring 1, hydroxyl addition reaction prefers to happen on the non-substituted carbons. Among all the reactions, the hydroxyl addition to C(2′) (pathway 11) is the easiest to occur for its lowest reaction energy barrier (0.20 kcal/mol) and high exothermic energy (16.86 kcal/mol). C(6′) has almost the same environment with C(2′). The only difference is that C(2′) is near to ring 1. This structure difference caused pathway 15 to overcome slightly higher reaction barrier (0.32 kcal/mol) than pathway 11.

Spin contamination at the MPWB1K optimized geometries has been examined. Take P1 (a doublet radical) for example, the calculated spin eigenvalues,<$S^{**}2$>, are reduced to 0.7507, 0.7503 and 0.8701 for MPWB1K, B3LYP and MP2 methods at the 6-311+G(d,p) basis set, respectively. Apparently, DFT method hardly shows spin contamination as the value for a pure doublet is 0.75, while MP2 emerged significant spin contamination. The MP2 method also predicts much higher energy barrier than DFT methods for each elementary reaction. The energies at B3LYP/6-311+G(3df,2p) and MP2/6-311+G(3df,2p) level are available at Table S1 in Supporting Information.

3.2. Frontier molecule orbital analysis

In order to characterize the reaction properties, frontier orbital theory is employed with concern about the highest occupied molecular orbital and lowest unoccupied molecular orbital of the reactants. The molecular orbital are examined at the MPWB1K/6-31+G(d,p) level. The shape of all the referred orbital plotted in Fig. 3. Hydroxyl radical has a lone pair of electrons at O atoms. The single occupied molecular orbital of OH radical lies on the lone electron pair of p orbital of O atom. Apparently, LUMO and LUMO+1 orbital of R(BDE7) is mainly localized on the p orbital of bromine and carbon atoms of ring 1. HOMO and HOMO-2 orbital are mainly focused on p orbital of atoms of ring 2 while ring 1 contributes most of HOMO-1. The relative energy is 161.20 kcal/mol between LUMO and HOMO orbital while that of LUMO and HOMO-1, LUMO and HOMO-2 are 171.15 and 178.22 kcal/mol, respectively. Generally, the reaction activities of R and OH radicals are predicted to be electron transformation from HOMO, HOMO-1 and HOMO-2 orbital of R to SOMO orbital of OH radical.

3.3. Kinetic properties

Canonical variational transition state theory (CVT), with small curvature tunneling (SCT) correction, has been successfully performed for the reaction of OH with BDE47. The error correction of the kinetic calculation is done using the small curvature tunneling (SCT) method. The theory has been used in this study to calculate the rate constants of the initial reactions over the temperature range of 200–1000 K.

To obtain the average error of the computational rate constants and experimental rate constants, we have calculated the rate constants for of at the MPWB1K/6-311+G(3df,2p)//MPWB1K/6-31+G(d,p) level by CVT/SCT method. The calculated rate constant is 6.58×10^{-15} cm^3 molecule^{-1} s^{-1}, which is 0.14×10^{-15} cm molecule^{-1} s^{-1} lower than the experiment value(6.66×10^{-15} cm^3 molecule^{-1} s^{-1})[44]. This suggest that CVT/SCT method is suitable for calculate rate constants.Jonathan D. Raff and Ronald A. Hites detected gas-phase rate constants for reaction of OH with several PBDEs with 0–2 bromine.[24] Zetzsch C. and coworkers detected rate constants for 2,2′,4,4′,5,5′-hexabromodiphenyl ether with OH radicals on aerosol [45]. Previous calculated rate constants by CVT/SCT method have been proved to give satisfy results. Our previous result of BDE-47 with OH radicals is 8.29×10^{-13} cm^3 molecule^{-1} s^{-1} at 298 K [22]. In fact, the abstraction of phenyl hydrogen has been confirmed to occur with quite low rate constants. In this paper, we calculated the rate constant for the title reactions to be 3.76×10^{-12} cm^3 molecule^{-1} s^{-1} at 298 K. This value is in well consistent with the reference value ($3.88^{+0.87}_{-0.71} \times 10^{-12}$ cm^3 molecule^{-1} s^{-1}, 298 K)[24].

These values are in consistent with the mechanism results. The rate-temperature formulas are fitted in Arrhenius Formulas:

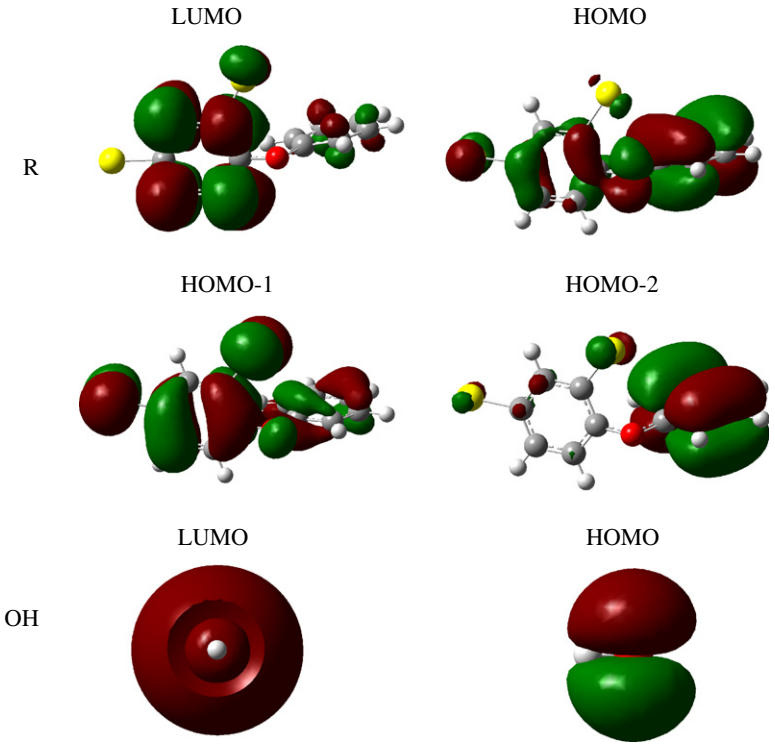

Fig. 3. Frontier molecular orbital of the BDE-7 and hydroxyl radical.

$$k = A\exp(-E/T) \quad (3)$$

The parameters (pre-exponential factor and activation energy) of each elementary step are shown in Table 1. Positive temperature dependences of the discussed rate constants can be seen in Table 2. For the multichannel reaction of OH with BDE-7, the overall OH-addition reaction rate constants of ring 1 and ring 2 are denoted as k_1 and k_2, respectively. The total rate constant for the OH+BDE-7 reaction is noted as k_a, where $k_a = k_1 + k_2$. The branch ratios for the whole reaction are k_1/k_a and k_2/k_a. Their branching ratios of each ring are also presented in Table 2. It seems that ring 2 plays a dominant role over the range of 200–1000 K. Fig. 4 has shown the theoretical rate constants (k_a) in this study and experiment values (k_{exp}, k_{max}, k_{min}) calculated through Arrhenius Formulas[24]. The average error between k_a and k_{exp} within the studied temperatures is 6.28×10^{-13} at the temperature of 200–500 K.

Based on the total rate constants at 298 K, the atmospheric lifetime τ has been calculated through the formula $\tau = 1/k_a[OH]$. [OH] is the atmospheric concentration of hydroxyl radicals which has been detected to be 9.7×10^5 molecule cm^{-3} [46]. Thus the atmospheric lifetime is 3.2 days.

Table 1
Rate constants calculated using CVT/SCT theory for the title reaction in the range of 200–1000 K.

	A	E	298 K	R
k_1	8.95×10^{-14}	517.73	1.58×10^{-14}	0.004
k_2	1.12×10^{-12}	6376.26	5.71×10^{-22}	1.52×10^{-10}
k_3	5.06×10^{-13}	515.04	8.99×10^{-14}	0.024
k_4	1.21×10^{-12}	6293.14	8.15×10^{-22}	2.17×10^{-10}
k_5	7.52×10^{-13}	470.94	1.55×10^{-13}	0.041
k_6	5.91×10^{-13}	539.83	9.66×10^{-14}	0.026
k_{10}	9.06×10^{-13}	468.31	1.88×10^{-13}	0.050
k_{11}	4.36×10^{-12}	278.04	1.72×10^{-12}	0.457
k_{12}	6.95×10^{-13}	485.58	1.36×10^{-13}	0.036
k_{13}	9.82×10^{-13}	485.92	1.93×10^{-13}	0.051
k_{14}	5.56×10^{-13}	482.17	1.10×10^{-13}	0.029
k_{15}	4.41×10^{-12}	425.92	1.06×10^{-12}	0.282

Table 2
Rate constants of k_1, k_2, total rate constants k, and the branching ratios of k_1/k and k_2/k.

T (K)	k_1	k_2	k	k_1/k	k_2/k
200	3.57×10^{-13}	3.40×10^{-12}	3.76×10^{-12}	0.095	0.905
300	3.61×10^{-13}	3.43×10^{-12}	3.79×10^{-12}	0.095	0.905
400	5.49×10^{-13}	4.64×10^{-12}	5.19×10^{-12}	0.106	0.894
500	7.06×10^{-13}	5.58×10^{-12}	6.29×10^{-12}	0.112	0.888
600	8.36×10^{-13}	6.32×10^{-12}	7.16×10^{-12}	0.117	0.883
700	9.42×10^{-13}	6.91×10^{-12}	7.85×10^{-12}	0.120	0.880
800	1.03×10^{-12}	7.39×10^{-12}	8.42×10^{-12}	0.122	0.878
900	1.11×10^{-12}	7.79×10^{-12}	8.90×10^{-12}	0.125	0.875
1000	1.17×10^{-12}	8.12×10^{-12}	9.30×10^{-12}	0.126	0.874

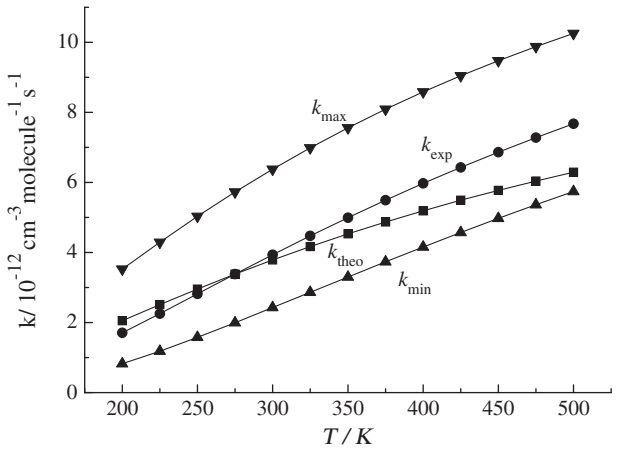

Fig. 4. Theoretical rate(k_a) constants and experiment rate constants(k_{exp}) between the temperature from 200 to 500 K. k_{max} is the highest detected values while k_{min} is the lowest values detected by Ref. [24].

4. Conclusions

Photochemical remove of PBDEs is thought to be important for the abundance radicals in atmosphere. Especially, hydroxyl radical is expected to react with PBDEs in huge amount. In this paper, BDE-7 has been selected as a represent of PBDEs for obtaining detailed information about the title reaction. First order reactions of BDE-7 with hydroxyl radical in atmosphere were detailed in this paper. Reaction rate constants were computed using CVT/SCT theory. The conclusions are drawn as follows:

(1) Two types of reactions, the addition of OH radical to BDE-7 and the hydrogen abstraction, were observed. The calculated results show that hydroxyl addition reaction is more predominant than abstraction reaction. Furthermore, the reaction that happened on ring 2 is more favorable than that occurred on ring 1. Among all the reactions (pathway 1–20), the hydroxyl addition to ortho position of ring 2 (pathway 11 and 15) is the most favorable. This phenomenon is also observed in the reactions of OH with phenol and cresol isomers where ortho position to the hydroxyl group is activated.

(2) The calculated rate constants show that OH radicals are likely to react with BDE-7 through addition reaction. The rate constant of the addition reaction is nearly an order magnitude higher than that of abstraction ones. Also, the total rate constant of ring 2 is larger than that of ring 1. At 298 K, the total rate constant of the title reaction is 3.76×10^{-12} cm^3 molecule^{-1} s^{-1} which is in well consistent with the experimental value of Raff and Hites [24]. Still, ring 2 contributes 82% to the total rate constants.

(3) Compared to the other PBDE reaction with OH radicals [22,23], we can see that the rate constant of BDE-7 is higher than that of BDE-47 [22], but is lower than the value of BDE-15 [23]. All the rate constants show positive temperature dependence in the range of discussed temperatures.

Acknowledgements

This work was supported financially by the National Natural Science Foundation of China (NSFC Nos. 21077067, 20877049, 21073220). Independent Innovation Foundation of Shandong University (IIFSDU, Project No. 2009JC016). We thank Professor Donald G. Truhlar for providing the POLYRATE 9.3 program.

Appendix A. Supplementary material

Supplementary data associated with this article can be found, in the online version, at doi:10.1016/j.comptc.2011.12.017.

References

[1] N.G. Dodder, B. Strandberg, R.A. Hites, Concentrations and spatial variations of polybrominated diphenyl ethers and several organochlorine compounds in fishes from the northeastern United States, Environ. Sci. Technol. 36 (2002) 146–151.
[2] R.A. Hites, Polybrominated diphenyl ethers in the environment and in people: a meta-analysis of concentrations, Environ. Sci. Technol. 38 (2004) 945–956.

[3] T.A. McDonald, A perspective on the potential health risks of PBDEs, Chemosphere 46 (2002) 745–755.
[4] R.A. Hites, Electron impact and electron capture negative ionization mass spectra of polybrominated diphenyl ethers and methoxylated polybrominated diphenyl ethers, Environ. Sci. Technol. 42 (2008) 2243–2252.
[5] R.A. Hites, J.A. Foran, S.J. Schwager, B.A. Knuth, M.C. Hamilton, D.O. Carpenter, Global assessment of polybrominated diphenyl ethers in farmed and wild salmon, Environ. Sci. Technol. 38 (2004) 4945–4949.
[6] M. Petreas, D. Nelson, F.R. Brown, D. Goldberg, S. Hurley, P. Reynolds, High concentrations of polybrominated diphenylethers (PBDEs) in breast adipose tissue of California women, Environ. Int. 37 (2011) 190–197.
[7] A. Mazdai, N.G. Dodder, M.P. Abernathy, R.A. Hites, R.M. Bigsby, Polybrominated diphenyl ethers in maternal and fetal blood samples, Environ. Health Persp. 111 (2003) 1249–1252.
[8] X.H. Bi, W.Y. Qu, G.Y. Sheng, W.B. Zhang, B.X. Mai, D.J. Chen, L. Yu, J.M. Fu, Polybrominated diphenyl ethers in South China maternal and fetal blood and breast milk, Environ. Pollut. 144 (2006) 1024–1030.
[9] S.S. Streets, S.A. Henderson, A.D. Stoner, D.L. Carlson, M.F. Simcik, D.L. Swackhamer, Partitioning and bioaccumulation of PBDEs and PCBs in Lake Michigan, Environ. Sci. Technol. 40 (2006) 7263–7269.
[10] J.P. Wu, X.J. Luo, Y. Zhang, Y. Luo, S.J. Chen, B.X. Mai, Z.Y. Yang, Bioaccumulation of polybrominated diphenyl ethers (PBDEs) and polychlorinated biphenyls (PCBs) in wild aquatic species from an electronic waste (e-waste) recycling site in South China, Environ. Int. 34 (2008) 1109–1113.
[11] J. Chevrier, K.G. Harley, A. Bradman, M. Gharbi, A. Sjodin, B. Eskenazi, Polybrominated diphenyl ether (PBDE) flame retardants and thyroid hormone during pregnancy, Environ. Health Persp. 118 (2010) 1444–1449.
[12] J. Legler, A. Brouwer, Are brominated flame retardants endocrine disruptors?, Environ Int. 29 (2003) 879–885.
[13] C.T. Chou, Y.C. Hsiao, F.C. Ko, J.O. Cheng, Y.M. Cheng, T.H. Chen, Chronic exposure of 2,2′,4,4′-tetrabromodiphenyl ether (PBDE-47) alters locomotion behavior in juvenile zebrafish (Danio rerio), Aquat. Toxicol. 98 (2010) 388–395.
[14] P.B. Key, K.W. Chung, J. Hoguet, B. Shaddrix, M.H. Fulton, Toxicity and physiological effects of brominated flame retardant PBDE-47 on two life stages of grass shrimp, Palaemonetes pugio, Sci. Total Environ. 399 (2008) 28–32.
[15] R.G. Ellis-Hutchings, G.N. Cherr, L.A. Hanna, C.L. Keen, The effects of marginal maternal vitamin a status on penta-brominated diphenyl ether mixture-induced alterations in maternal and conceptal vitamin a and fetal development in the sprague dawley rat, birth defects research Part b-developmental and reproductive, Toxicology 86 (2009) 48–57.
[16] Y.F. Jiang, X.T. Wang, K. Zhu, M.H. Wu, G.Y. Sheng, J.M. Fu, Occurrence, compositional profiles and possible sources of polybrominated diphenyl ethers in urban soils of Shanghai, China, Chemosphere 80 (2010) 131–136.
[17] J. Wang, M.M. Kliks, S. Jun, Q.X. Li, Residues of polybrominated diphenyl ethers in honeys from different geographic regions, J. Agric. Food. Chem. 58 (2010) 3495–3501.
[18] J. Eriksson, N. Green, G. Marsh, A. Bergman, Photochemical decomposition of 15 polybrominated diphenyl ether congeners in methanol/water, Environ. Sci. Technol. 38 (2004) 3119–3125.
[19] J.D. Raff, R.A. Hites, Deposition versus photochemical removal of PBDEs from lake superior air, Environ. Sci. Technol. 41 (2007) 6725–6731.
[20] L. Sanchez-Prado, C. Gonzalez-Barreiro, M. Lores, M. Llompart, C. Garcia-Jares, R. Cela, Photochemical studies of a polybrominated diphenyl ethers (PBDES) technical mixture by solid phase microextraction (SPME), Chemosphere 60 (2005) 922–928.
[21] G.M. Clifford, L.R. Thuner, J.C. Wenger, D.E. Shallcross, Kinetics of the gas-phase reactions of OH and NO3 radicals with aromatic aldehydes, J. Photochem. Photobiol. A-Chem. 176 (2005) 172–182.
[22] H.J. Cao, M.X. He, D.D. Han, Y.H. Sun, J. Xie, Theoretical study on the mechanism and kinetics of the reaction of 2,2′,4,4′-tetrabrominated diphenyl ether (BDE-47) with OH radicals, Atmos. Environ. 45 (2011) 1525–1531.
[23] J. Zhou, J.W. Chen, C.H. Liang, Q. Xie, Y.N. Wang, S.Y. Zhang, X.L. Qiao, X.H. Li, Quantum chemical investigation on the mechanism and kinetics of PBDE photooxidation by center dot OH: a Case study for BDE-15, Environ. Sci. Technol. 45 (2011) 4839–4845.
[24] J.D. Raff, R.A. Hites, Gas-phase reactions of brominated diphenyl ethers with OH radicals, J. Phys. Chem. A 110 (2006) 10783–10792.
[25] M.J. Frisch, G.W. Trucks, H.B. Schlegel, P.W.M. Gill, B.G. Johnson, M.A. Robb, J.R. Cheeseman, T.A. Keith, G.A. Petersson, J.A. Montgomery, K. Raghavachari, M.A. Allaham, V.G. Zakrzewski, J.V. Ortiz, J.B. Foresman, J. Cioslowski, B.B. Stefanov, A. Nanayakkara, M. Challacombe, C.Y. Peng, P.Y. Ayala, W. Chen, M.W. Wong, J.L. Andres, E.S. Replogle, R. Gomperts, R.L. Martin, D.J. Fox, J.S. Binkley, D.J. Defrees, J. Baker, J.P. Stewart, M. Head-Gordon, C. Gonzales, J.A. Pople, Gaussian 03. Gaussian, Inc., Wallingford, CT, 2003.
[26] B.J. Lynch, P.L. Fast, M. Harris, D.G. Truhlar, Adiabatic connection for kinetics, J. Phys. Chem. A 104 (2000) 4811–4815.
[27] X.H. Qu, H. Wang, Q.Z. Zhang, X.Y. Shi, F. Xu, W.X. Wang, Mechanistic and kinetic studies on the homogeneous gas-phase formation of PCDD/Fs from 2,4,5-trichlorophenol, Environ. Sci. Technol. 43 (2009) 4068–4075.
[28] X.H. Qu, Q.Z. Zhang, W.X. Wang, Theoretical study on NO_3-initiated oxidation of acenaphthene in the atmosphere, Canadian J. Chem. Revue Canadienne De Chimie 86 (2008) 129–137.
[29] F. Xu, H. Wang, Q.Z. Zhang, R.X. Zhang, X.H. Qu, W.X. Wang, Kinetic properties for the complete series reactions of chlorophenols with OH radicals-relevance for dioxin formation, Environ. Sci. Technol. 44 (2010) 1399–1404.
[30] Q.Z. Zhang, S.G. Li, X.H. Qu, X.Y. Shi, W.X. Wang, A Quantum mechanical study on the formation of PCDD/Fs from 2-chlorophenol as precursor (vol 42, pg 7301, Environ. Sci. Technol. 44 (2010) (2008) 3645.
[31] Q.Z. Zhang, S.Q. Li, X.H. Qu, X.Y. Shi, W.X. Wang, A quantum mechanical study on the formation of PCDD/Fs from 2-chlorophenol as precursor, Environ. Sci. Technol. 42 (2008) 7301–7308.
[32] Q.Z. Zhang, X.H. Qu, H. Wang, F. Xu, X.Y. Shi, W.X. Wang, Mechanism and thermal rate constants for the complete series reactions of chlorophenols with H, Environ. Sci. Technol. 43 (2009) 4105–4112.
[33] Q.Z. Zhang, X.H. Qu, W.X. Wang, Mechanism of OH-Initiated atmospheric photooxidation of dichlorvos: a quantum mechanical study, Environ. Sci. Technol. 41 (2007) 6109–6116.
[34] Q.Z. Zhang, W.N. Yu, R.X. Zhang, Q. Zhou, R. Gao, W.X. Wang, Quantum chemical and kinetic study on dioxin formation from the 2,4,6-TCP and 2,4-DCP precursors, Environ. Sci. Technol. 44 (2010) 3395–3403.
[35] W. Yu, J. Hu, F. Xu, X. Sun, R. Gao, Q. Zhang, W. Wang, Mechanism and direct kinetics study on the homogeneous gas-phase formation of PBDD/Fs from 2-BP, 2,4-DBP, and 2,4,6-TBP as precursors, Environ. Sci. Technol. 45 (2011) 1917–1925.
[36] C. Gonzalez, H.B. Schlegel, Reaction path following in mass-weighted internal coordinates, J. Phys. Chem. 94 (1990) 5523–5527.
[37] M.S. Baldridge, R. Gordor, R. Steckler, D.G. Truhlar, Ab initio reaction paths and direct dynamics calculations, J. Phys. Chem. 93 (1989) 5107–5119.
[38] B.C. Garrett, D.G. Truhlar, Generalized transition state theory: Classical mechanical theory and applications to collinear reactions of hydrogen molecules, J. Phys. Chem. 83 (1979) 1052–1079.
[39] A. Gonzalez-Lafont, T.N. Truong, D.G. Truhlar, Interpolated variational transition state theory: practical methods for estimating variational transition state properties and tunneling contributions to chemical reaction rates from electronic structure calculations, J. Chem. Phys. 95 (1991) 8875–8894.
[40] A.E. Fernandez-Ramos, B.A. Ellingson, B.C. Garret, D.G. Truhlar, Variational Transition State Theory with Multidimensional Tunneling, in: K.B. Lipkowitz, T.R. Cundari (Eds.), Reviews in Computational Chemistry, Wiley-VCH, Hoboken, NJ, 2007.
[41] R. Steckler, Y.Y. Chuang, P.L. Fast, J.C. Corchade, E.L. Coitino, W.P. Hu, G.C. Lynch, K. Nguyen, C.F. Jackells, M.Z. Gu, I. Rossi, S. Clayton, V. Melissas, B.C. Garrett, A.D. Isaacson, D.G. Truhlar, POLYRATE Version 9.3, University of Minnesota: Minneapolis, 2002.
[42] J.D. Cox, D.D. Wagman, V.A. Medvedev, CODATA Key Values for Thermodynamics, Hemisphere, New York, 1989 (1989).
[43] B. Ruscic, R.E. Pinzon, M.L. Morton, N.K. Srinivasan, M.C. Su, J.W. Sutherland, J.V. Michael, Active thermochemical tables: Accurate enthalpy of formation of hydroperoxyl radical, HO_2, J. Phys. Chem. A 110 (2006) 6592–6601.
[44] V.L. Orkin, S.N. Kozlov, G.A. Poskrebyshev, M.J. Kurylo, Rate constant for the reaction of OH with H-2 between 200 and 480 K, J. Phys. Chem. A 110 (2006) 6978–6985.
[45] C. Zetzsch, W.-U. Palm, H.-U. Kruger, Photochemistry of 2,2′,4,4′,5,5′-hexaBDE (BDE-153) in THF and adsorbed on SiO2: first observation of OH reactivity of BDEs on aerosol, Organohalogen Compd. 66 (2004) 2281–2287.
[46] R.G. Prinn, R.F. Weiss, B.R. Miller, J. Huang, F.N. Alyea, D.M. Cunnold, P.J. Fraser, D.E. Hartley, P.G. Simmonds, Atmospheric trends and lifetime of CH3CCI3 and Global OH concentrations, Science 269 (1995) 187–192.